GOMOS OZONE PROFILE VALIDATION USING DATA FROM GROUND-BASED AND BALLOON-SONDE MEASUREMENTS

Y. J. Meijer[(1)], D. P. J. Swart[(1)], M. Allaart[(2)], S. B. Andersen[(3)], G. Bodeker[(4)], I. Boyd[(5)], G. Braathen[(6)], Y. Calisesi[(7)], H. Claude[(8)], V. Dorokhov[(9)], P. von der Gathen[(10)], M. Gil[(11)], S. Godin-Beekmann[(12)], F. Goutail[(13)], G. Hansen[(14)], A. Karpetchko[(15)], P. Keckhut[(13)], H. M. Kelder[(2)], R. Koelemeijer[(1)], B. Kois[(16)], R. M. Koopman[(17)], J.-C. Lambert[(18)], T. Leblanc[(19)], I. S. McDermid[(19)], S. Pal[(20)], G. Kopp[(21)], H. Schets[(22)], R. Stubi[(23)], T. Suortti[(15)], G. Visconti[(24)], and M. Yela[(11)]

(1) National Institute for Public Health and the Environment (RIVM), Postbus 1, 3720 BA Bilthoven, The Netherlands, Yasjka.Meijer@rivm.nl; Daan.Swart@rivm.nl; Robert.Koelemeijer@rivm.nl
(2) Royal Netherlands Meteorological Institute, De Bilt, The Netherlands, allaart@knmi.nl; kelder@knmi.nl
(3) Danish Meteorological Institute, Copenhagen, Denmark, sba@dmi.dk
(4) National Institute of Water and Atmospheric Research, Lauder, New Zealand, g.bodeker@niwa.co.nz
(5) University of Massachusetts & National Institute of Water and Atmospheric Research, Amherst (MA), USA, boyd@fcrao1.astro.umass.edu
(6) Norwegian Institute for Air Research, Kjeller, Norway, geir@nilu.no
(7) Institute of Applied Physics, Bern, Switzerland, yasmine.calisesi@issi.unibe.ch
(8) Deutscher Wetterdienst, Hohenpeissenberg, Germany, Hans.Claude@dwd.de
(9) Central Aerological Observatory, Moscow, Russia, vdor@caomsk.mipt.ru
(10) Alfred Wegener Institute for Polar and Marine Research, Potsdam, Germany, gathen@awi-potsdam.de
(11) Instituto Nacional de Técnica Aeroespacial, Torrejon de Ardoz, Spain, gilm@inta.es; yelam@inta.es
(12) Centre National de la Recherche Scientifique, Paris, France, sophie.godin@aero.jussieu.fr
(13) Centre National de la Recherche Scientifique, Verrieres-le-Buisson, France, fgoutail@aerov.jussieu.fr; philippe.keckhut@aerov.jussieu.fr
(14) Norwegian Institute for Air Research, Tromso, Norway, ghh@nilu.no
(15) Finnish Meteorological Institute, Sodankylä, Finland, alex.karpetchko@fmi.fi; tuomo.suortti@fmi.fi
(16) Institute of Meteorology and Water Management, Warsaw, Poland, bogdan.kois@imgw.pl
(17) ESA-ESRIN, Via Galileo Galilei, I-00044 Frascati, Italy, Rob.Koopman@esa.int
(18) Belgian Inst. for Space Aeronomy (BIRA), Avenue Circulaire 3, Bruxelles, Belgium, j-c.lambert@iasb.be
(19) Jet Propulsion Laboratory, Wrightwood (CA), USA, leblanc@tmf.jpl.nasa.gov; mcdermid@tmf.jpl.nasa.gov
(20) Meteorological Service of Canada, Toronto, Canada, shiv@yorku.ca
(21) Institut für Meteorologie und Klima-forschung - Forschungszentrum Karlsruhe, Karlsruhe, Germany, kopp@imk.fzk.de
(22) Royal Meteorological Institute (RMI), Ringlaan 3, Brussels B-1180, Belgium, henk.schets@oma.be
(23) Meteo Swiss, Payerne, Switzerland, rsi@meteoswiss.ch
(24) University of L'Aquila, L'Aquila, Italy, guido.visconti@aquila.infn.it

ABSTRACT

One of the nine instruments on-board the polar-orbiting environmental satellite ENVISAT is the Global Ozone Monitoring by Occultation of Stars (GOMOS) instrument. This paper presents validation results of GOMOS ozone profiles (v6.0a) from comparisons to microwave radiometer, balloon ozonesonde and lidar measurements worldwide. Thirty-one instruments/ launch-sites at twenty-five stations ranging from the Arctic to the Antarctic joined in this activity. We identified 3,713 useful collocated observations that were performed within an 800-km radius and a maximum 20-hours time difference of a satellite observation, for the period June 2002 and March 2003. These collocated profiles were compared and the results were analyzed for possible dependencies on several geophysical (e.g., latitude) and GOMOS observational (e.g., star characteristics) parameters. In a dark atmospheric limb the GOMOS data agree very well with the correlative data and between 20- to 61-km altitude their differences only show a small (2.5%) insignificant negative bias with a standard deviation of about 14%. This conclusion is demonstrated to be independent of the star temperature and magnitude, and the latitudinal region of the GOMOS observation.

1. INTRODUCTION

In March 2002 the European Space Agency (ESA) has launched ENVISAT with on-board the Global Ozone Monitoring by Occultation of Stars (GOMOS) instrument. This instrument exploits the stellar occultation technique for the detection of atmospheric ozone and other trace gases, as well as temperature [1]. The technique allows the acquisition of spatially high-resolution atmospheric transmission spectra, and its principle is based on the changing spectrum of a light

Proceedings of the Second Workshop on the Atmospheric Chemistry Validation of ENVISAT (ACVE-2)
ESA-ESRIN, Frascati, Italy, 3-7 May 2004 (ESA SP-562, August 2004) EGO01YM

source observed outside and through the Earth's atmosphere. Using the acquired spectra and the known molecular cross-sections, the vertical trace-gas profiles are retrieved.

Validation of ENVISAT instruments is performed in several subgroups of the Atmospheric Chemistry Validation Team (ACVT). This paper on the validation of GOMOS ozone profiles is a joint contribution of the Ground-based Measurement and Campaign Database (GBMCD) subgroup. For the GOMOS Cal/Val-team it is very important to get unanimous recommendations on the quality of their product. Therefore within the GBMCD subgroup, we have centralized the analysis of the data involving ozone profile measurements. In addition, we hope to be able to extract some information on the global validity of the product.

An initial geophysical validation campaign has been carried out during the first nine months after launch. The preliminary validation results of this campaign were presented during the ENVISAT validation workshop from 9-12 December 2002 in Frascati, Italy. This paper forms a continuation and extension of the work presented by Meijer et al. [2] on the joint GBMCD validation results of GOMOS ozone profiles.

In the next section we will briefly present the origin of the data used in the analysis and the criteria applied for defining a collocated measurement. In section 3 we present the analysis of the GOMOS data compared to the GBMCD data with respect to several important GOMOS measurement parameters. Finally in section 4, we present the conclusions and the recommendations.

2. DATA

2.1 GBMCD data

The Ground-Based Measurement and Campaign Database (GBMCD) subgroup of the Atmospheric Chemistry and Validation Team (ACVT) provides correlative data from ground-based instruments and small balloons. For comparison to GOMOS ozone profiles, we received 847 profiles from nineteen sonde launch stations, 508 profiles from eight lidar stations, and 849 daily files from four microwave radiometer (MWR) stations.

Validation of data implies the use of reliable correlative data with known (high) quality for the analysis. Here we have used data from networks with regular validation activities, such as the Network for the Detection of Stratospheric Change (NDSC; www.ndsc.ws).

To ensure quality further, the altitude ranges of the three different instruments are restricted to those ranges where known optimal quality and highest altitude resolution prevails. Based on this, we have chosen to use sonde data between 0- and 30-km, lidar data between 18- and 45-km, and MWR data between 30- and 70-km altitude. In addition, the maximum allowed error is 30% for the lidar and MWR data. For the sonde data, a similar restriction could not be applied due to the absence of a reported ozone error.

The GBMCD subgroup enfolds several different instruments at several geolocations. In Table 1 we have listed all the AO-teams that have contributed to this paper and also which instruments were involved. For a more detailed description of each project we refer to the project proposals.

2.2 GOMOS data

The GOMOS data analyzed here have been generated with ESA's prototype processor version 6.0a at ACRI (Sophie-Antipolis, France). Although the data availability dramatically improved compared to the situation for the ACVT workshop in December 2002, we still miss about 45% of the requested data. Nevertheless, this unavailability did not hamper the assessment presented here, as will become clear later.

As GOMOS data contain profiles with varying quality, we have removed data with a reported error above 20%, which is a good quality filter. Furthermore, we required the ozone data to be between 0 and 10^{19} molecules/m^3. In addition, we imposed a consistency in the profile by requiring that over a 2-km interval at least 80% of the neighboring data points should also be accepted. The remaining profile should also cover at least a 4-km range interval, otherwise it is completely rejected.

As became clear previously, the GOMOS data quality suffers from the illumination condition of the atmospheric limb in which the star sets. For the analysis of the ACVE-2, the validation teams were requested to only focus on GOMOS measurements performed in a dark atmospheric limb. Apart from the obvious division between measurements on the day- and nightside of the ENVISAT orbit, there is also a transition area, see Table 2. In the v6.0a processed data, this area is divided into three subselections, namely twilight, straylight and straylight&twilight conditions. A twilight limb condition is defined as the situation when the solar zenith angle (SZA) at the geolocation of the tangent point is between 90^{o} and 110^{o}. A straylight condition is defined as the situation when the SZA at the geolocation of the ENVISAT platform is between 0^{o} and 110^{o}. Inherent to the ENVISAT orbit, this straylight condition occurs in the Arctic region. Note that in Table 2 the three states of the transition area are summed up and called 'Twilight'.

Table 1. Overview and details of stations and instruments providing correlative data. The details also include the network affiliation, the ESA AO-project number and the principle investigator (PI) of the instrument.

Location	Latitude	Longitude	Instrument	Profiles	AO-id	Instrument PI-name	Institute
Ny-Ålesund (P)	78.92	11.93	Lidar	115	331	P. von der Gathen	AWI
Ny-Ålesund (P)	78.92	11.93	Sonde	74	331	P. von der Gathen	AWI
Thule (P)	76.53	-68.74	Sonde	26	158	S. Andersen	DMI
Scoresbysund (C)	70.48	-21.97	Sonde	34	158	S. Andersen	DMI
Alomar (C)	69.30	16.00	Lidar	54	9079	G. Hansen	NILU
Kiruna (C)	67.84	20.41	Microwave	103	191	U. Raffalski	IRF
Sodankylä (C,W)	67.37	26.63	Sonde	78	429	E. Kyrö	FMI
Keflavik	64.00	-22.00	Sonde	25	191	M. Gil	INTA
Orland	63.40	9.20	Sonde	19	158	A. Vik	NILU
Yakutsk (C)	62.02	129.63	Sonde	4	158	V. Dorokhov	CAO
Jokioinen (W)	60.81	23.50	Sonde	27	429	E. Kyrö	FMI
Legionowo (C)	52.40	20.97	Sonde	48	174	B. Kois	IMWM
De Bilt (C,W)	52.10	5.18	Sonde	47	174	M. Allaart	KNMI
Uccle (C,W)	50.80	4.35	Sonde	114	300	D. De Muer	RMIB
Hohenpeissenberg (C,W)	47.80	11.02	Lidar	24	360	H. Claude	DWD
Hohenpeissenberg (C,W)	47.80	11.02	Sonde (BM)	32	360	H. Claude	DWD
Payerne (C,W)	46.82	6.95	Sonde	113	158	R. Stubi	MeteoSwiss
Payerne (C)	46.82	6.95	Microwave	275	158	N. Kaempfer	MeteoSwiss
Obs. Haute Provence (P)	43.94	5.71	Lidar	83	360	S. Godin-Beekmann	CNRS
Toronto (C)	43.66	-79.4	Lidar	5	153	S. Pal	MSC
L'Aquila	42.34	13.33	Sonde	3	206	G. Visconti	UNIVAQ
Table Mountain (C)	34.40	-117.70	Lidar	76	360	I. S. McDermid	JPL
Mauna Loa (P)	19.54	-155.58	Lidar	87	360	I. S. McDermid	JPL
Mauna Loa (P)	19.54	-155.58	Microwave	257	179	A. Parrish	UMass & NIWA
Paramaribo (C,W,S)	5.75	-55.20	Sonde	39	174	M. Allaart	KNMI
Lauder (P)	-45.04	169.68	Lidar	64	9003	D. Swart	RIVM & NIWA
Lauder (P)	-45.04	169.68	Microwave	214	179	A. Parrish	UMass & NIWA
Lauder (P)	-45.04	169.68	Sonde	57	179	G. Bodeker	NIWA
Marambio (W)	-64.20	-56.70	Sonde	42	429	E. Kyrö	FMI
Dumont d'Urville (P)	-66.67	140.01	Sonde	27	158	F. Goutail	CNRS
Belgrano	-78.00	-38.00	Sonde	28	191	M. Yela	INTA

(P): NDSC primary station (Network for the Detection of Stratospheric Change)
(C): NDSC complementary station
(W): WOUDC station (World Ozone and Ultraviolet Radiation Data Center)
(S): SHADOZ station (Southern Hemisphere Additional Ozonesondes)
(BM): Brewer/Mast ozonesonde type

Although we have been requested to only assess the pure dark limb occultations, we have performed our analysis on the occultations measured when the SZA exceeded 108 ^{o} at the geolocation of the tangent point. In Table 2 we show the differences in the number of selected profiles when applying these different criteria. The number in brackets indicates the number of cases arising from our pure dark limb definition.

2.3 Collocation criteria

As the correlative instruments did not exactly sample the same atmosphere as the satellite instrument, in order to compare the GOMOS to the GBMCD ozone profiles, we defined criteria that allow a maximum temporal and spatial difference of respectively 20-hours and 800-km. From the available GOMOS and GBMCD data that fulfill these and previously mentioned quality

Table 2. Statistics of used GOMOS profiles and the influence of applying different selection criteria.

Selection	Day-light	Twi-light	Dark	All	Dark & Twilight
Available	1706	1540	467	3713	2007
Bad points	72%	25%	16%	45%	24%
Bad profiles	682	6	1	689	7
No overlap	362	32	4	398	36
Useful	662	1502	462	2626	1964 (1387)

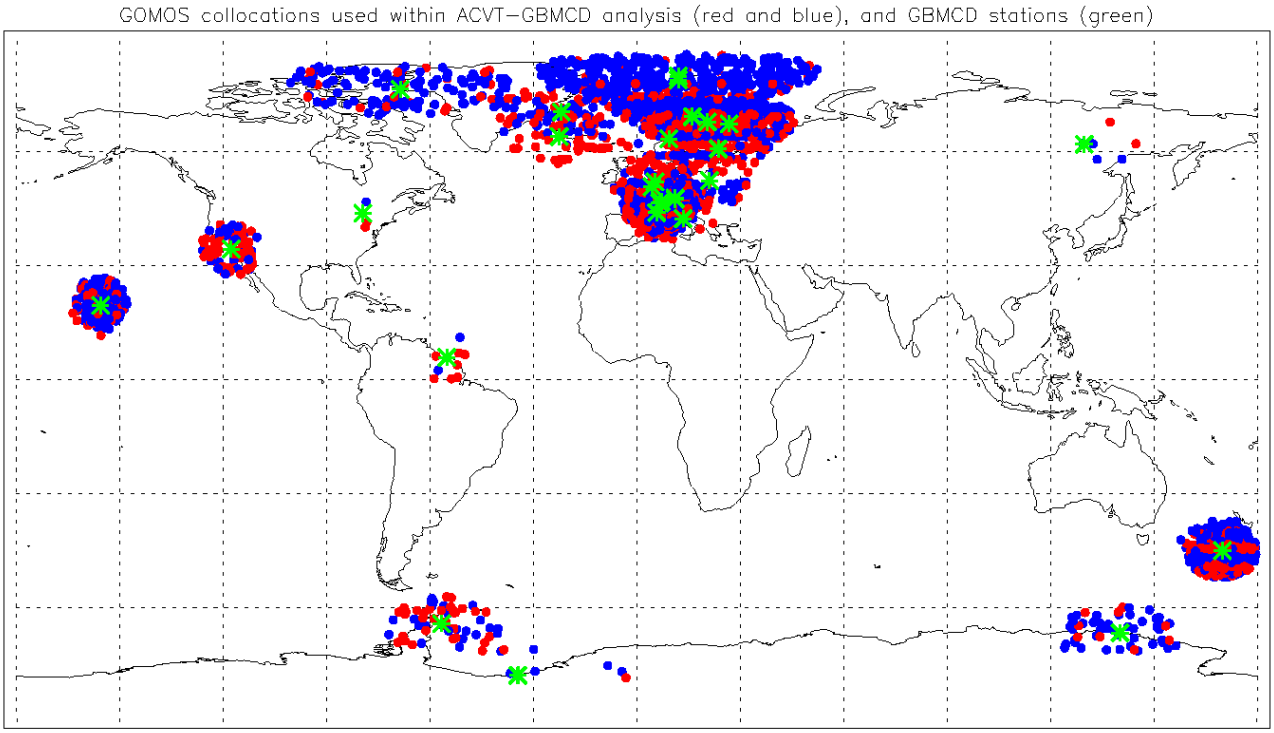

Fig. 1. Geolocations of all 3,713 available GOMOS measurements collocated (in time and space) with data from the contributing measurement stations (green asterisks). Distinction has been made between measurements made in bright limb (red dots), and twilight or dark limb (blue dots). Data shown were measured within an 800-km radius and a maximum 20-hours time difference of a GBMCD observation. Remarkable is the sparse availability of GOMOS data around the (tropical) Paramaribo and (Antarctic) Belgrano stations, which is despite their on average data provision (see Table 1).

requirements, we could identify 1,387 useful collocated profile pairs measured in dark limb condition. Note that, due to accurate planning of the balloon-sonde and lidar observations, the collocation criteria relate to maximum differences. Since in the lower and middle mesosphere there is a strong diurnal variation in the ozone profile, we required a maximum time difference of 5-hours for all the data pairs measured above 50-km altitude. An overview of the geolocation of all the 3,713 GOMOS measurements used in the analysis is shown in Fig. 1, which is plotted together with the station geolocations of the GBMCD data.

3. ANALYSIS

The aim of this paper is to assess the GOMOS ozone profile quality and check for possible dependencies on certain parameters, such as the brightness and temperature in the large ensemble of targeted stars. The quality in the lower stratosphere is expected to be determined by the star magnitude, whilst at higher altitudes the star's temperature is more important, as hot stars produce significant emission in the UV part of the spectrum. We also check whether the obliquity of the occultation influences the results. The parameter used, to differentiate the results for this, is the line-of-sight (LOS) angle with respect to the anti-flight direction of ENVISAT, hereafter referred to as LOS angle. Apart from the measurement-related parameters, the analysis is also performed with respect to the latitude band and the applied collocation criteria. In Table 3 we list the selections as used in the analysis, which are all based on the selection using our own dark limb definition (see top entry Table 3).

Table 3. Analysis parameters and their ranges used in the GOMOS ozone profile quality assessment.

Parameter	**Selection range**	**Selection name**
Atmos. limb, SZA	>108^o	Dark
Star vis. magnitude	-2 to +1	Strong
	+1 to +4	Weak
Star temp. (K)	1,000 to 7,000	Cold
	7,000 to 50,000	Hot
Star LOS angle	-10 to +10	Back
	+10 to +45	Slant
	+45 to +90	Side
Latitude region	0^o-23.5^o	Tropical
	23.5^o-66.5^o	Mid-latitude
	66.5^o-90^o	Polar
Collocation criteria	800 km, 20 hrs	Default
	400 km, 10 hrs	2x Stricter
	200 km, 5 hrs	4x Stricter

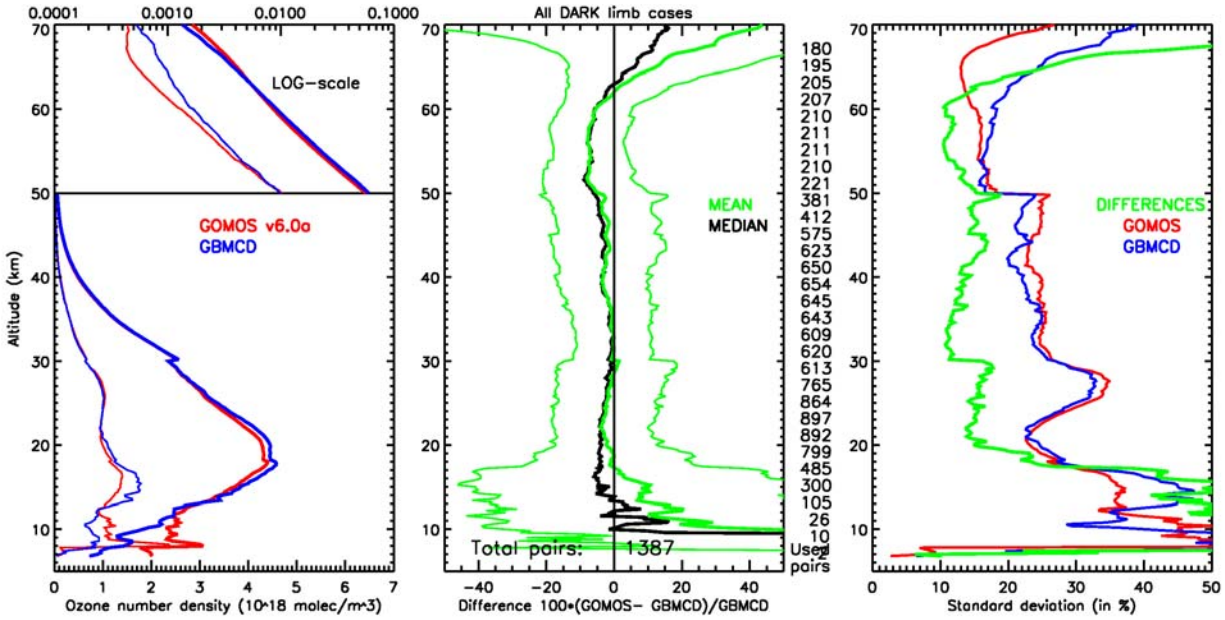

Fig. 2. Intercomparison results of paired data in which GOMOS measured in dark atmospheric limb condition. Left panel shows the mean of the GOMOS (bold red line) and GBMCD (bold blue line) ozone profiles and their standard deviations (thin lines). Middle panel shows their mean (green line) and median (black line) differences, including the standard deviation of the differences (thin line). Right panel shows the standard deviation of the differences (green line), and of the GOMOS (red line) and GBMCD (blue line) ozone profiles.

3.1 Comparison approach

The differences in retrieved measurement units have been accounted for by transforming all data to values of ozone number density versus geometric altitude. To be able to compare both profile sets, we have linearly interpolated all profiles to a common altitude grid with 200-m intervals.

From the set of collocated pairs, or any subset of them, we calculate the mean and the standard deviation of the GOMOS and GBMCD ozone profiles. In addition, we calculate the mean, the standard deviation, and the median of their differences; calculated as GOMOS minus GBMCD data in percentage relative to the latter. Per altitude level the availability of valid data pairs is evaluated (i.e., is there overlap in altitude), and only from these data points we derive all of the above quantities.

3.2 Results of all dark limb occultations

In Fig. 2 we present the analysis results for the collocated pairs in which GOMOS measured in a dark atmospheric limb. The discontinuities in the left panel profiles (e.g., at 30-km altitude) originate from the differences in the number of used pairs per altitude level, which are partly due to the GBCMD-data altitude restrictions. Note that data from different instruments are not always measured in the same latitudinal range or season, and hence these discontinuities can be understood from geophysics. The analysis of all dark limb situations gives good results. Between 13- and 65-km altitude there are only minor systematic biases in the GOMOS ozone profile, which are between 0 and ±10%. The standard deviation of the differences is smaller than 20% between 19- and 63-km altitude.

3.2.1 Influence of star-related parameters

In Fig. 3 we present the selections investigating the influence of different star-related parameters. The top panels show the influence of the star temperature; all stars (left), hot stars (middle) and cold stars (right). The middle panels show the influence of the star visual magnitude; all stars (left), strong stars (middle) and weak stars (right). The bottom panels show the influence of the occultation obliqueness, expressed as the LOS angle; back angles (left), slant angles (middle) and side angles (right).

3.2.2 Influence of latitude region

In Fig. 4 we present the selections investigating the influence of latitude region. The top panels show the analysis results of GOMOS measurements in polar regions. Please note the small number of used pairs above 50-km altitude. The middle panels show the analysis results of GOMOS measurements in mid-latitude regions. The bottom panels show the analysis results of GOMOS measurements in tropical regions.

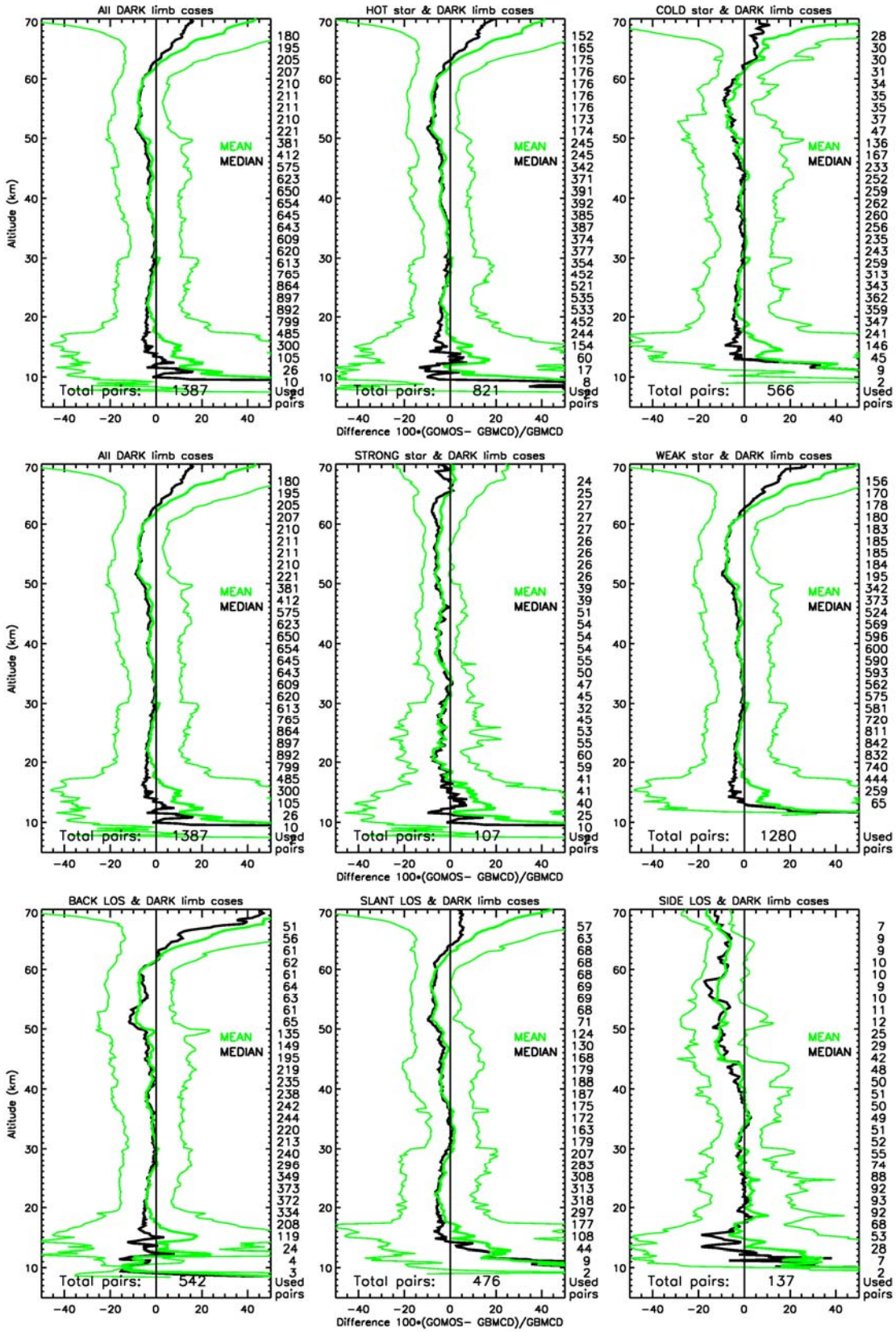

Fig. 3. Influence of star-related parameters on the analysis results; similar presentation as the middle panel of Fig. 2. The selections involve paired data in which GOMOS performed measurements observing stars with different temperatures (top), magnitudes (middle), and under different LOS angles (bottom), see Table 3 for definitions.

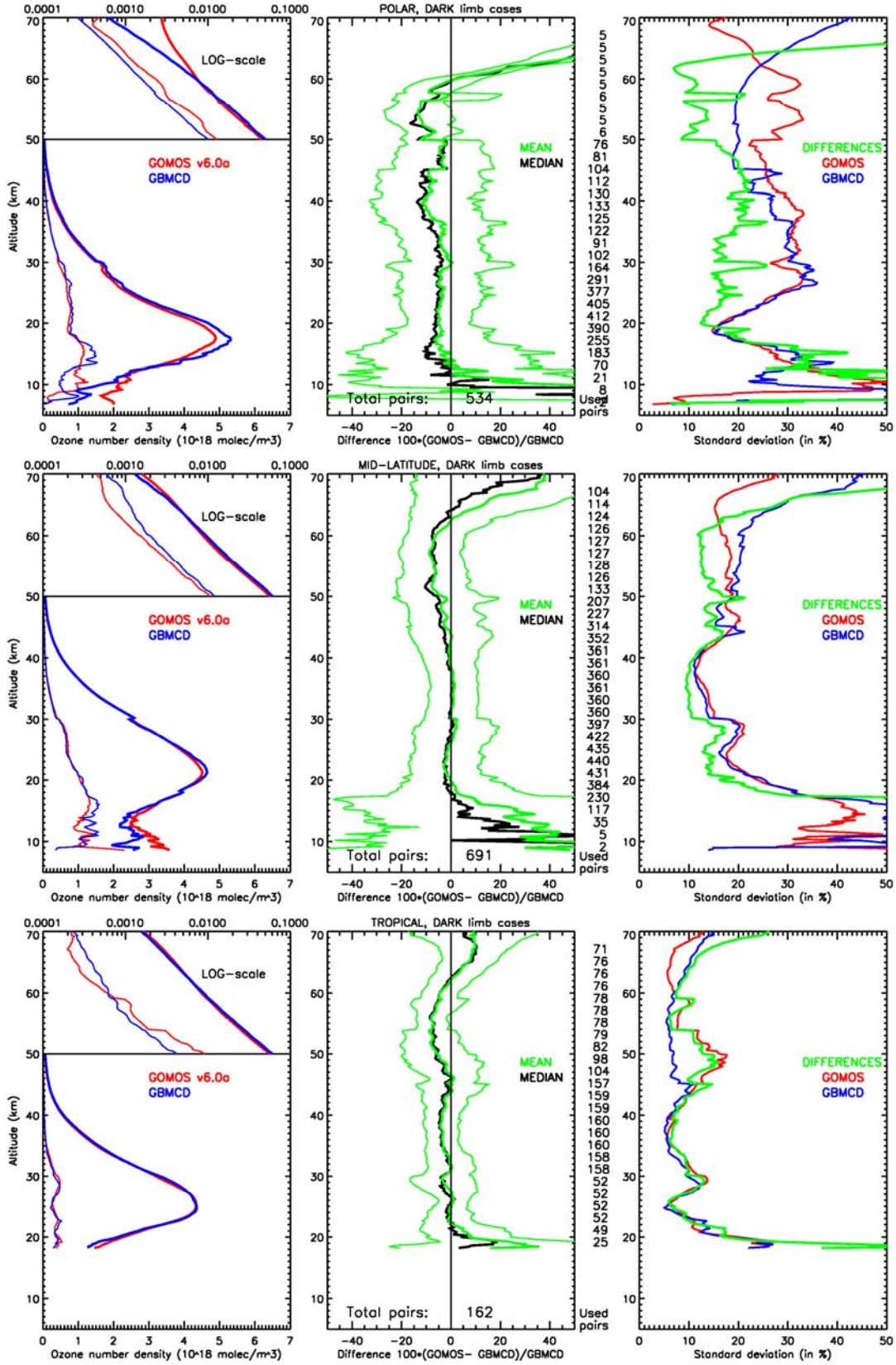

Fig. 4. Influence of latitude region on the analysis results; similar presentation as Fig. 2. The selections involve paired data in which GOMOS measured in dark limb condition and in polar (top), mid-latitude (middle) and tropical (bottom) regions (see Table 3 for definitions).

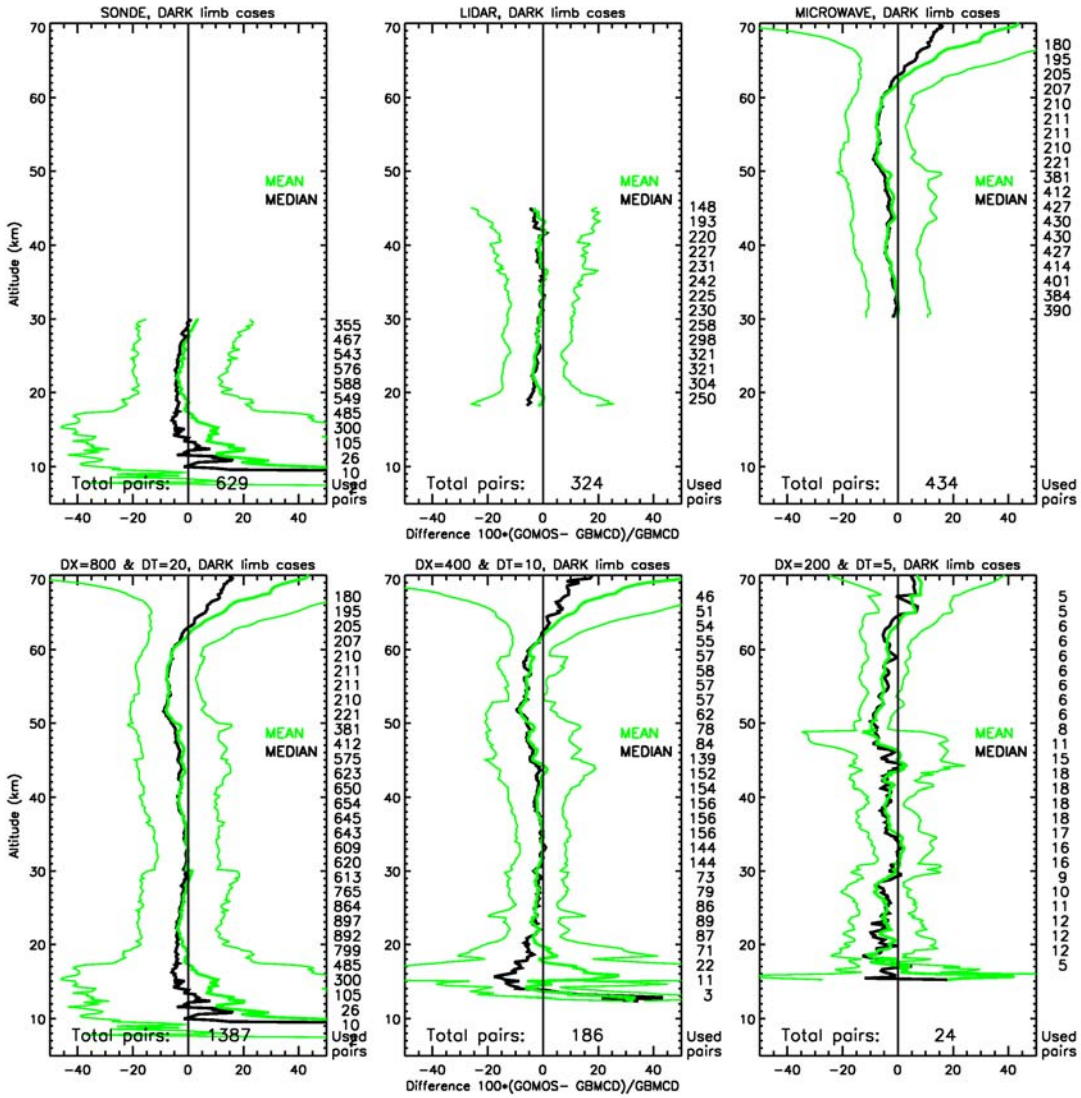

Fig. 5. The top panels show the influence of the used correlative instrument, and these selections only involve those data in which GOMOS data are paired with sonde (top left), lidar (top middle), and microwave data (top right). The bottom panels show the influence of the applied collocation criteria. GOMOS data are paired with GBMCD data using default (bottom left), twice stricter (bottom middle), and four times stricter (bottom right) collocation criteria in both space and time, see Table 3 for definitions. Note that above 50-km altitude the time criterion is always 5 hrs.

3.2.3 Influence of GBMCD instrument

In the top panels of Fig. 5 we present the selections investigating the influence of the used correlative instrument. The panels show the analysis results involving GOMOS data paired with sonde (left), lidar (middle) and MWR (right) data. The analysis results show a very consistent picture for each type of instrument.

3.2.4 Influence of collocation criteria

In the bottom panels of Fig. 5 we present the selections investigating the influence of the applied collocation criteria. The observed biases for the different selections are very similar. Although the standard deviation of the differences improves, also the number of pairs decreases drastically which limits the possibility for the investigation of subselections.

4. CONCLUSIONS

The data from the ACRI prototype processor seem to have no significant biases for the occultations measured under dark limb conditions, i.e., SZA greater than 108^{o}. Therefore, at the moment we can not think of any objections to release the GOMOS data measured under these circumstances. The standard data processor of ESA needs to be upgraded to comply with the status of the prototype processor. In the quality assessment of

these profiles we have shown that between 13- and 65-km altitude there is a very small negative bias, which is within 10% of the GBMCD ozone profiles. The standard deviation of the differences between the GOMOS and GBMCD profiles is within 20% between 19- and 63-km altitude. The GBMCD profiles used in this analysis were measured both in the southern and northern hemisphere. Above 63-km altitude the analysis results are likely to be influenced by the quality of the MWR data, which reach their maximum altitude range.

There is no significant influence on the analysis results resulting from the temperature or magnitude of the tar used in the GOMOS observation. Note that data points with a large error bar have been filtered out, which is reflected in the smaller number of pairs in the higher altitude range for the cold star selection. Data resulting from stars observed under side LOS angles give worse results above 50-km altitude.

In polar regions the analysis results show a slightly larger negative bias, especially between 35- and 45-km altitude. Results with no bias are obtained between 25- and 45-km altitude in mid-latitude regions.

Furthermore, we have demonstrated that the results have no significant dependence on the used correlative instrument or the applied collocation criteria.

More detailed conclusions and a thorough discussion of the analysis results have been submitted to JGR [3] and the reader is referred to that reference for more information.

5. REFERENCES

1. Bertaux, J. L., et al., Monitoring of Ozone Trend by Stellar Occultations: The GOMOS Instrument, *Adv. Space Res.*, Vol. 11, No. 3, 237-242, 1991.

2. Meijer, Y. J., et al., Analysis of GOMOS ozone profiles compared to GBMCD datasets (bright/dark, star magnitude, star temperature), *Proc. of ENVISAT Validation Workshop* (Frascati, Italy, 9-12 December 2002), ESA SP-531, 2003.

3. Meijer, Y. J., et al., Pole-to-pole validation of ENVISAT/GOMOS ozone profiles using data from ground-based and balloon-sonde measurements, *J. Geophys. Res.*, 2004JD004834, submitted 2004.

6. ACKNOWLEDGEMENTS

We greatly appreciate the support and feedback given by the GOMOS quality working group, and the prompt feedback from the people at ACRI for the GOMOS data processing using ESA's prototype processor. The institutes contributing to the GOMOS mission and this working group are ACRI, Service d'Aeronomie, Finnish Meteorological Institute, Belgian Institute for Space Aeronomy, Atrium Space, ECMWF, and from the European Space Agency ESRIN-PCF, ESOC and ESTEC-PLSO.

This research was partly funded by a grant from the User Support Program managed by the program bureau external research of the Space Research Organization Netherlands (PB-SRON). Most of the data used in this publication was obtained as part of the Network for the Detection of Stratospheric Change (NDSC) and is publicly available (see http://www.ndsc.ws). The authors would like to thank ESA and the NILU Cal/Val team for providing data through the ENVISAT Cal/Val database. The standard data format greatly enhances the accessibility for these kinds of large-scale validation activities incorporating multiple datasets. In addition, we would like to acknowledge the tremendous effort of our co-workers involved in measuring, processing and uploading all the correlative measurements.

We are grateful to the following agencies and institutes for their financial support to part of the GBMCD measurements used in this study: ASI (Italy), CNES (France), CSA (Canada), DMI (Denmark), ESA, European Union, Federaal Wetenschapsbeleid (Belgium), INSU (France), IPEV (France), MeteoSwiss (Switzerland), MSC (Canada), NASA, NIVR (The Netherlands), NIWA (New Zealand), and SNF (Denmark).